geoconvention
Calgary • Canada • May 15-17 2023

Microseismic monitoring using SADAR arrays at the Newell County carbon storage facility: what have we learned in a year?

Kevin D. Hutchenson, PhD
Derek Quigley
Jamie Longbow, PhD.
Elige "Buck" Grant, PhD
Paul Nyffenegger PhD
Jason Jennings
Mark Tinker, PhD
Quantum Technology Sciences, Inc.

Mike Dahl
David Grindell
Geospace Technologies Canada, Inc.

Don C. Lawton, PhD
Marie Macquet, PhD
University of Calgary, Carbon Management Canada (CMC)

Introduction

Common and traditional methods or techniques to monitor small magnitude seismicity, or microseismicity, even man-made seismic events, is with the use of passive surface or downhole sensors. However, we have found surface sensors to be limited due to a low signal-to-noise ratio even though they may cover a wide spatial area. Most downhole sensors are used with available wells, deploying sensors along the outer casing at some range of depths. As such, they may offer limited coverage of the field (Eaton, 2018, 136).

Our approach is to deploy phased arrays (Zhang *et al.*, 2023) at some depth. Two dimensional (planar) arrays have been deployed at depth for many years as an aid to global and regional monitoring, especially for the longer wavelengths associated with large events (Rost and Thomas, 2002). Quantum Technology Sciences, Inc. (Quantum) has developed a 3D array to incorporate several 2D planar sections at depth and built to incorporate higher frequency data associated with surveillance and industrial sources. As it happens, these 3D compact, volumetric, phased array systems (SADAR arrays) work well for microseismic applications, especially with the co-produced three-dimensional beamforming and spatially coherent processing used to optimally suppress non-coherent and coherent noise from directions other than the main response axis (MRA) for a beam of interest.

The microseismic application includes data from the Newell County CO_2 storage facility, monitored by the Containment and Monitoring Institute at the Newell County Facility (NCF) to test and demonstrate technologies for CO_2 injection/storage (Macquet *et al.*, 2022; Lawton *et* *al.*, 2019). The NCF was constructed to provide a methodological approach to CO_2 injection, capture, migration exploration, and as a testbed for technologies to be investigated via monitoring, simulation, and modeling.

Four SADAR arrays were installed in mid-November of 2021 at distances between 70 and 300 m from the injection site (Figure 1). Since that time, they have been continuously operating, recording events associated or a result of the injection process. In addition, many events are recorded whose contribution appears related to site activity at the surface, both within the compound and in the neighboring area. For example, vibroseis units operating during active surveys are easily detected. A few events have been found from arriving from outside the immediate area, including some low frequency, narrow band events from the west, and apparent ice breakage in the lake to the east. Cultural events, such as moving vehicles on nearby roads, are also detected, and can be tracked.

The arrays consist of multiple cylindrical shells of multiple dimensions representing three different shapes (Zhang *et al.*, 2023). Sensor counts for the various designs range between 51 and 72 sensors. Sensors are buried from 9 m to 19 m, depending on the array and number of layers.

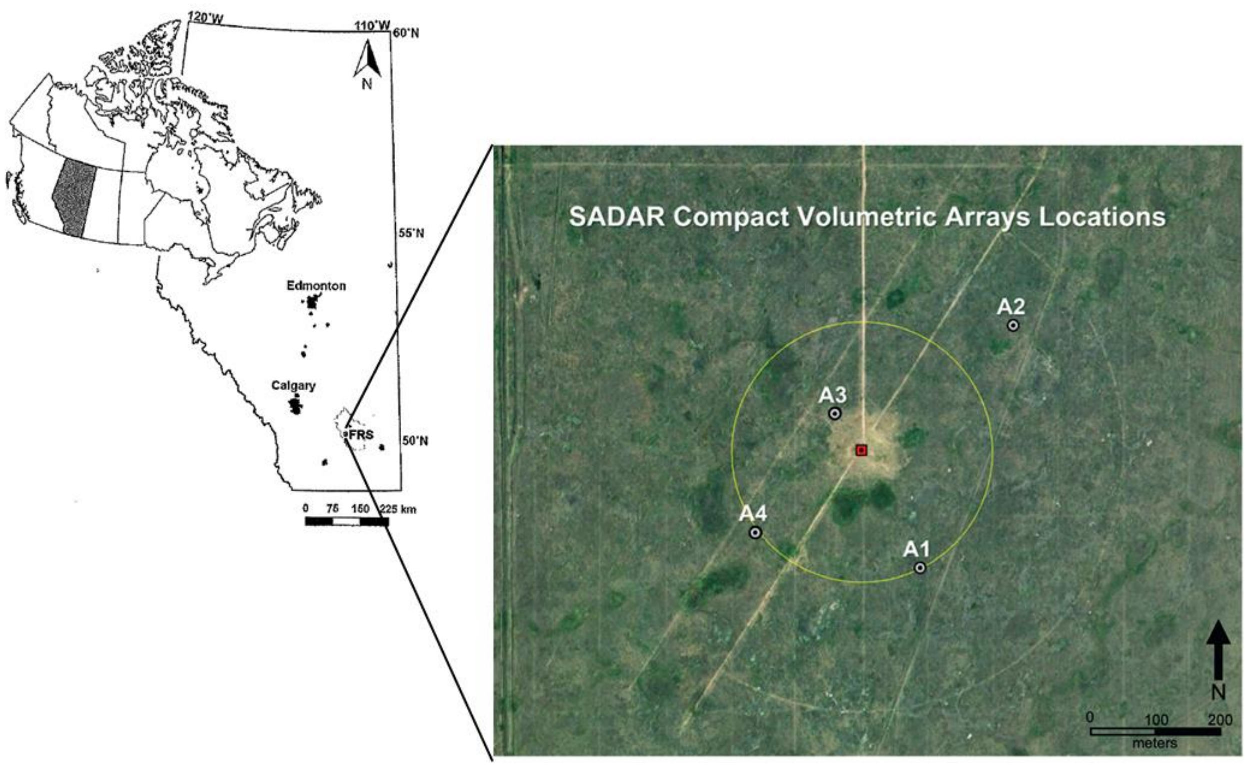

Figure 1. A map view showing NCF with respect to Alberta, and a close-up view of the site with the injection well (red square) and four SADAR arrays marked A1 to A4. The yellow circle represents 200 m from the injection well (adapted from Lawton *et al.*, 2019 and Nyffenegger *et al.*, 2022).

The event processing workflow includes data preconditioning (*e.g.*, windowing, filtering, and FK beamforming), 4D scanning (event detection), relocation, and moment magnitude calculations (Zhang *et al.*, 2022). Observed energy of a typical microseismic event arrives first as P-wave energy across the whole network. The SNR is improved by taking advantage of the phased array and constructing the optimal beam at each array. This allows low SNR arrivals to be detected and picked more precisely. In addition, by running a full-waveform source scanning (Kao and Shan, 2004) over time and space (*e.g.*, 10m x 10m spatial grids and 5-sec sliding time window) using the whole array network and travel-time look-up-tables, potential events emerge with high semblance (stack of model-aligned energy transient/onset, *e.g.*, STA/LTA). Events above a threshold become the initial set of detected events. Each initial detection is associated with a best-matched grid point in space and serves as the initial location input for a relocation process based on an iterative non-linear inversion using the arrival-time picks and optional FK attributes (*e.g.*, azimuth). A standard least-square location algorithm is used which simultaneously solves for all event locations and station corrections (Bratt and Bache, 1988). This results in more accurate relative locations. Known ground truth is supplied by known artificial events at the surface and one pseudo-calibration event at depth, allowing the near surface and deeper layers of the velocity model to be improved. Moment magnitude is calculated by using the displacement spectrum based on the Brune (1970, 1971) source model following Shearer (2009).

Results and Observations

Following a year of monitoring, from November 2021 to mid-December 2022, approximately 1800 events were detected and located using three or more arrays. This list was scrubbed to only include events observed at all four of the arrays (563 events). Care was taken to remove suspect events resulting from human activity at the surface (events with a zero depth). The compound has a lot of traffic, resulting in many shallow impulsive events. The remainder consists of a well-scrubbed bulletin of approximately 200 events.

The 200 events were reviewed by a human analyst to refine the phase onset times for each of the four arrays and to determine the *deltim* for each phase onset time. The *deltim* represents the uncertainty of the phase onset; the sharper the onset time, the smaller the *deltim*, and smaller errors in the location. In addition, each of the station magnitudes were reviewed to assure the best fit of the source model.

Figure 2 shows the spatial and depth orientation of these events. Spatially, most of the events are within -100 m to 100 m of the injection well, a few events further out. The events are generally distributed above 150 m with a few events between 150 m to 200 m depth. This patten agrees with previous observations at this facility.

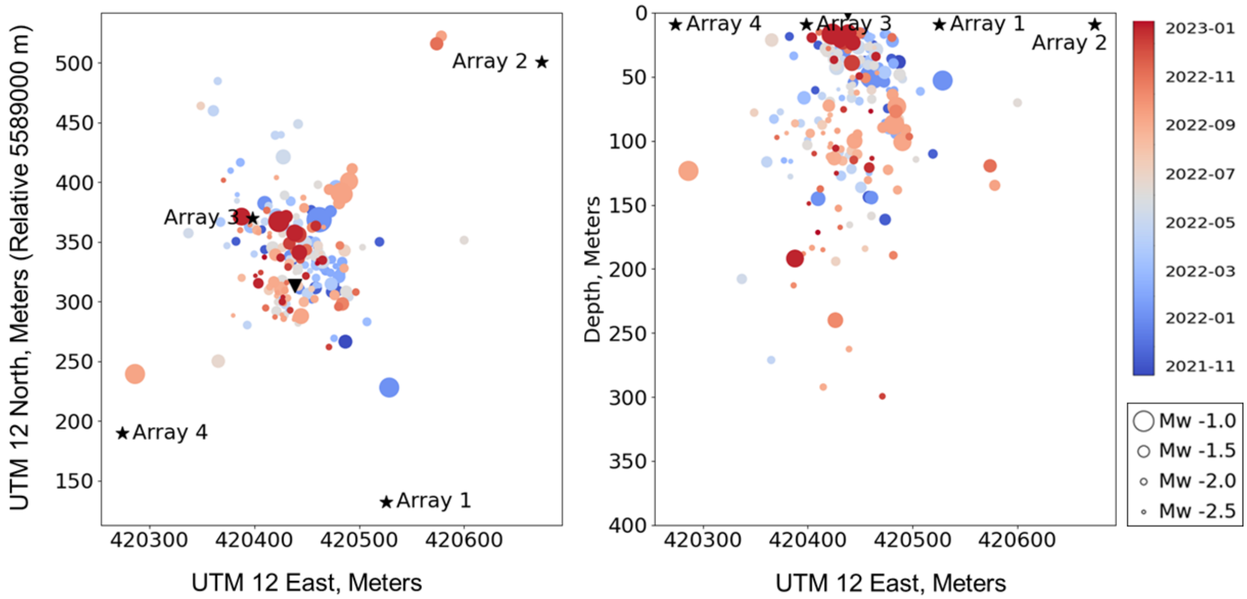

Figure 2. A map view and cross section from east to west of the NCF showing the spatial and depth location of the events observed from all four arrays. Events are chronology color-coded and sized relative to magnitude. For orientation, the locations of all four arrays are shown (black stars) with the injection well as a black triangle. The spatial dimensions are meters in UTM zone 12N; the depth is in meters.

Surface injection points at different points within NCF have allowed calibration of the shallow seismic velocities used in the location. An artificial event from swabbing one of the observation wells created an opportunity to calibrate the deeper seismic velocities. With these calibration events, relative location uncertainty has been achieved for many of the events on the order of 10 m.

Following Brune (1970, 1971), moment magnitudes were calculated for each of the events. The approach is to calculate the magnitudes at each station with a displacement spectrum fit using the Brune model, then averaging across the four arrays to obtain a network magnitude. The spectral fits are made on unfiltered data but using a least-squares fit between 10 and 90 Hz. Many of the magnitudes are best fit between bands of 30 and 90 Hz. Figure 3 illustrates the bin of network magnitudes for this group of well-located events.

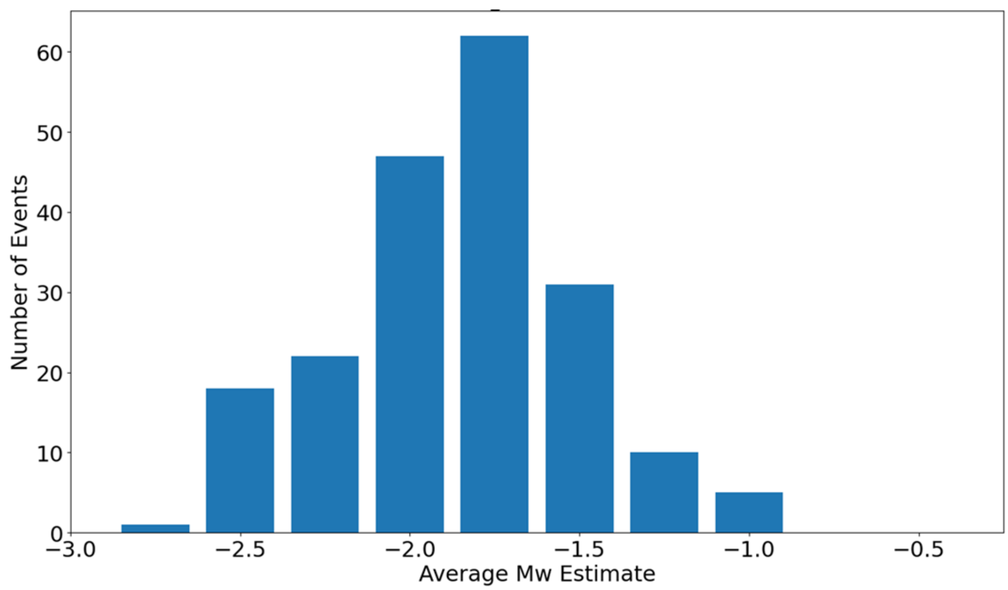

Figure 3. Distribution of event network Mw over the course of the year.

A magnitude-distance scatter plot can show a detection-distance bias for the area. The Mw values at each station. plotted versus distance in Figure 4 show a bi-modal distribution caused by the proximity of array A3 (closest to the injection well and the primary source zone) compared to the more distant arrays A1, A4, and A2. The dashed lines reflect integer signal-to-noise (SNR) levels between 1 and 5 following the equation by Zimmer (2011). This scenario suggests the detection SNR is around 2 for the farthest arrays (>150 m). For the closest arrays (< 150 m) the plot suggests the smallest events may not be resolvable with the surface noise (Eaton, 2018).

Not all events recorded by the SADAR system were from the immediate area. Some occur outside the immediate area. These events are not included in the bulletin.

Traffic along roads to the west and north of the NCF have been recorded and tracked. The array architecture allows the beam MRA to point to coherent energy from any direction. The azimuth from the MRA as a function of time allows a coherent track to be constructed, thus the ability to track vehicles on roads near the site.

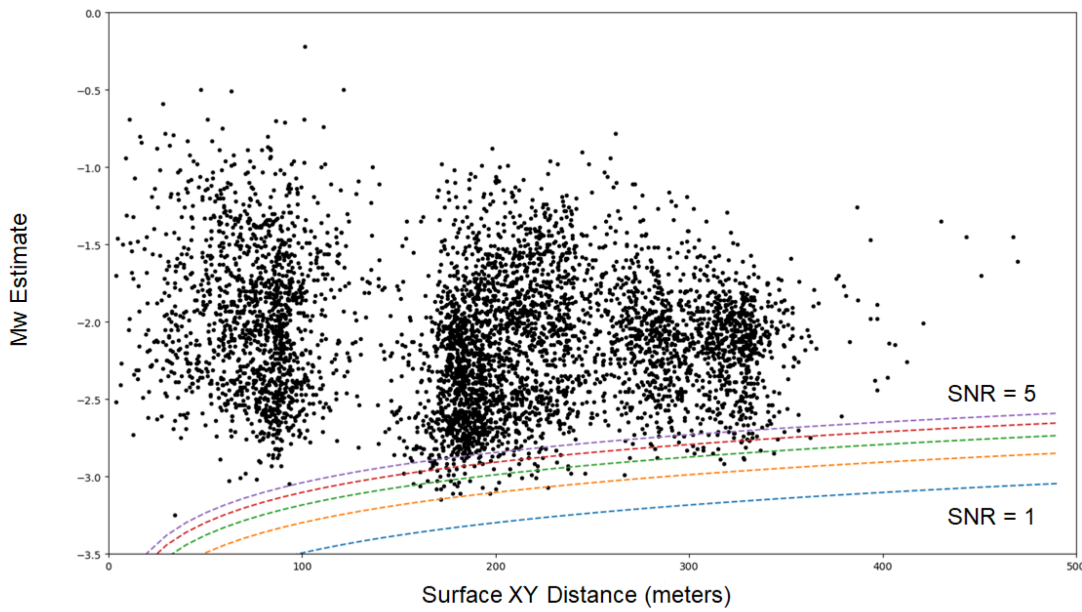

Figure 4. Magnitude (Mw) vs. distance for the station magnitudes. The family of lines represent the SNR levels 1-5 (Zimmer, 2011).

In addition, low frequency energy (16-20 Hz) has been observed arriving from a westerly direction. It is clearly outside the NCF; no known origin or source has been associated to date. The aperture across the network does not allow for a good triangulation solution for energy sources far outside of the network.

During the late Winter and early Spring, ice on the canal and lake to the east was breaking up. Numerous shallow impulsive events originated from this location. These were relatively small, isochromatic events.

Conclusions

Monitoring the microseismicity at the NCF has demonstrated how compact, volumetric, phased array system networks such as the SADAR system can contribute to routine monitoring for seismicity associated with carbon CO2 injection and storage. In addition, there is now an analyst reviewed bulletin from which future studies can use as a baseline for comparison with when reservoir engineering activities switch to larger volumes and higher injection pressures, with automated evaluating bulletins from automated processing pipelines, and with for evaluating additional other instrumentation networks at the NCF, to name but a few. Furthermore, Quantum intends to maintain and expand the bulletin for the foreseeable future, which will allow longer-term patterns in the seismicity to be identified, as well as documenting seismicity changes as engineering activities alter the reservoir and cap-rock at the NCF.

Acknowledgements

Quantum Technology Sciences, Inc., is a wholly owned subsidiary of Geospace Technologies Corporation, Inc. We acknowledge CMC for providing access to the Newell County Facility to enable installation of the SADAR system, and for sharing the data from the surface and downhole networks. The Newell County Facility is supported by funding from the Global Research Initiative at the University of Calgary from the Canada First Research Excellence Fund and from the Containment and Monitoring Institute Joint Industry Project. CMC is also acknowledged for providing operational data from the site.

References

Bratt, S.R. and T.C. Bache, 1988, Locating events with a sparse network of regional arrays, Bull. Seism. Soc. Am., **78**(2), 780-798.

Brune, J., 1970, Tectonic stress and the spectra of seismic shear waves from earthquakes, JGR, **75**, 4997-5009.

Brune, J., 1971, Correction, JGR, **76**, 5002.

Eaton, D., 2018, Passive seismic monitoring of induced seismicity, Cambridge University Press, New York.

Kao, H. and Shan, S.-J., 2004. The source-scanning algorithm: mapping the distribution of seismic sources in time and space, Geophysical Journal International, **157**(2), 589-594.

Lawton, D. C., J. Dongas, K. Osadetz, A. Saeedfar, and M. Macquet, 2019, Chapter 16: Development and analysis of a geostatic model for shallow CO2 injection at the Field Research Station, Southern Alberta, Canada: in T. Davis, M. Landrø, and M. Wilson, eds., Geophysics and Geosequestration: Cambridge University Press, 280-296, DOI3

Macquet, M., D. Lawton, K. Osadetz, G. Maidment, M. Bertram, K. Hall, B. Kolkman-Quinn, J. Monsegny Parra, F. Race, G. Savard, Y. Wang, 2022, Overview of Carbon Management Canada's pilot-scale CO2 injection site for developing and testing monitoring technologies for carbon capture and storage, and methane detection: Recorder Focus Article, **47**, No. 01, April 2022.

Nyffenegger, P. A., M. A. Tinker, J. Zhang, E. B. Grant, K. D. Hutchenson, and D. C. Lawton, 2022, Compact phased arrays for microseismic monitoring: First Break, **40**, 69-74.

Rost, S. and C. Thomas, 2002, Array seismology: methods and applications, Rev. Geophys., **40**(3), 2-1—2.27.

Shearer, P., 2009, Introduction to Seismology, Cambridge University Press, New York.

Zhang, J., K.D. Hutchenson, P.A. Nyffenegger, E.B. Grant, P.A. Nyffenegger, E.B. Grant, J. Jennings, M.A. Tinker, M. Macquet, and D.C. Lawton, 2023, Performance comparison of compact phased arrays and traditional seismic networks for microseismic monitoring at a CO2 sequestration test site, The Leading Edge, (accepted for publication).

Zhang, J., K.D. Hutchenson, P.A. Nyffenegger, M.A. Tinker, K.D. Hutchenson, and D.C. Lawton, 2022, Seismic monitoring using compact phased arrays, Part II: CO2 sequestration monitoring: presented at IMAGE, August, 2022.

Zimmer, U., 2011, Microseismic design studies, Geophysics, **76**(6), WC17-WC25.